Results in Engineering 28 (2025) 108155

Contents lists available at ScienceDirect

Results in Engineering

journal homepage: www.sciencedirect.com/journal/results-in-engineering

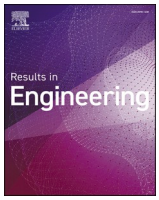

Research paper

Durability and life-cycle evaluation of high-plasticity clays treated with zeolite as partial replacement of cementitious stabilizers

Pouya Alipanahi [a], Paria Mirzaee [b], Majid Naghdipour Mirsadeghi [c], Farimah Fattahi Masrour [d], Farshad Yazdani [e], Jorge G. Zornberg [a], Hossein MolaAbasi [f,*]

[a] Department of Civil, Architectural and Environmental Engineering, University of Texas at Austin, Austin, TX, USA
[b] Sari University of Agricultural Sciences and Natural Resources, Mazandaran, Iran
[c] Department of Environmental Engineering, College of Environment, Karaj, Iran
[d] Department of Civil Engineering, University of Galway, Galway, Ireland
[e] Department of Civil Engineering, Sharif University of Technology, Azadi Ave., Tehran, Iran
[f] Department of Civil Engineering, Gonbad Kavous University, Golestan, Iran

ARTICLE INFO

Keywords:
Zeolite
Durability
Pressure wave velocity
Life cycle assessment
Road construction

ABSTRACT

The durability and mechanical properties of high-plasticity clay stabilized with a combination of cement and zeolite additives were evaluated after cycles of wet-dry conditions with the goal of identifying the optimal dosage of Zeolite for road construction. The accumulated loss of mass (*ALM*), pressure wave velocity (V_P), and constrained modulus (*CM*) were adopted as key parameters to assess the durability of soil mixtures. The *ALM* measures durability by weight loss during *W–D* cycles, while V_P and *CM* from ultrasonic tests were measured after each cycle to evaluate stiffness and strength. Results demonstrated that a 30 % replacement of lime by zeolite resulted in an optimal dosage to reduce *ALM* and increase V_P and *CM*. Furthermore, life cycle assessment and life cycle cost analyses revealed a substantial decrease in carbon emissions (up to 62 %), and cost savings (up to 54 %) could be reached with increased zeolite content in the mixture. These environmental and economic benefits support the Incorporation of zeolite into stabilizer mixtures for road construction. Finally, the results indicate that 30 % zeolite replacement enhances durability and mechanical properties and also contributes to sustainable and low-carbon construction. It is suggested that the research could benefit other fields in terms of using the concept of incorporating the stabilizing agent in the form of waste to make it more eco-friendly for construction activities, thus providing an economical means for construction with reduced carbon emissions.

1. Introduction

Pavement structures are particularly vulnerable to prolonged water infiltration, which presents a significant challenge to their long-term performance [1]. High-plasticity clays exhibit excessive moisture changes, and loss of strength, which compromise long-term pavement subgrade performance. Specifically, the infiltration of surface water into the water-sensitive layers of the pavement diminishes the resilient modulus and shear strength of these materials [2], causing relatively greater deflections in the pavement structure. These cover asphalt stripping in flexible pavements, soil pumping in rigid pavements, fine particle migration into drainage layers, and expansive clay subgrade expansive soils [3]. All these play a significant role in compromising long-term pavement performance. Conventional cement stabilization mitigates these effects, but at a significant cost of CO_2 emission. Zeolite, as a natural pozzolanic material with high silica and alumina content, may be employed for partial cement replacement and augmentation of strength, durability, and water resistance in high-plasticity clays with a sustainable stabilization alternative [4].

High plasticity clays may result in significant geotechnical problems, including those associated with volumetric changes triggered by variations in the water content. According to previous studies, approximately 12 % of the Earth's surface is covered by expansive soils, which exhibit an irregular distribution [5]. The high levels of smectite minerals, including montmorillonite, in high plasticity clays are one of the primary causes of deformations during Wetting-Drying (*W-D*) cycles [6].

* Corresponding author.
E-mail addresses: pouyaalipanahi@utexas.edu (P. Alipanahi), F.fattahimasrour1@universityofgalway.ie (F.F. Masrour), farshad.yazdani@sharif.edu (F. Yazdani), zornberg@mail.utexas.edu (J.G. Zornberg), hma@gonbad.ac.ir (H. MolaAbasi).

https://doi.org/10.1016/j.rineng.2025.108155
Received 9 September 2025; Received in revised form 27 October 2025; Accepted 9 November 2025
Available online 10 November 2025

Swell-shrink behavior plays a crucial role in the failures of structures such as pavements, low-rise buildings, and pipelines [7–10]. As a result, yearly recovery costs are estimated to be in the billions of dollars [11]. Expansive soils cause significant damage to infrastructure, with annual reconstruction and rehabilitation costs within the United States estimated at $10–15 billion, including nearly $6 billion for pavement structures alone. Total damages have increased by an estimated 160 % between 1990 and 2020, ranking expansive soils as one of the leading causes of infrastructure deterioration in both the U.S. and globally [12]. Studies have recently revealed that zeolite can be a sustainable and effective stabilizer for expansive clays, improving mechanical performance and controlling volumetric instability while reducing environmental impact [13].

Calcium-based materials like cement have traditionally been employed conventionally as stabilizers for the treatment of high plasticity clays, with success demonstrated for improved geotechnical properties [7,13,14]. However, in recent years, research has increasingly focused on more eco-friendly stabilizers like fly ash, ground granulated blast furnace slag, metakaolin, and geopolymer-based stabilizers, in an attempt to make the carbon footprint and costs associated with soil improvement more favorable [15]. Amongst these alternatives, natural zeolite appears to have garnered interest for imamts high SiO_2 to Al_2O_3 ratio, high cation-exchange capacity, and high pozzolan reactivity, which allow for the production of 'secondary *C-S-H* and *C-A-H* gel,' similar to those from traditional cement hydration [4,16]. Compared with other supplementary cementitious materials, the benefits offered by zeolites lie in their natural availability, low processing energy requirements, and potentially favorable costs with similar long-term increases in strengths with durability improvement benefits similar to those offered by ordinary supplementary cementitious materials alike [17]. Therefore, using these in road construction would make for frugal as well as eco-friendly approaches in stabilizing expansive clays with simultaneous reduced cement usage in road construction projects.

Soil stabilization using cementitious materials is a well-established approach to improve the strength and durability of weak soils for infrastructure applications; however, the production of cement required to meet global demand accounts for about 6–8 % of worldwide CO_2 emissions [18,19] and involves significant energy consumption, posing serious environmental challenges. The manufacture of cement involves the use of non-renewable resources and demanding industrial processes, such as crushing, heating, storing, and grinding the final product. Additionally, the heating stage requires temperatures exceeding 1650 °C [20], resulting in significant energy consumption and greenhouse gas emissions [21]. As an alternative to the use of cement, progress has been made towards the use of environmental materials to improve soil geotechnical characteristics, including vegetation [22,23], Microbial-Induced Carbonate Precipitation (*MICP*) [24] and Enzyme-Induced Carbonate Precipitation (*EICP*) [25].

To mitigate these issues, researchers have explored sustainable and low-carbon alternatives, particularly the partial replacement of cement with natural or industrial pozzolans. Among these, natural zeolite has received growing attention due to its high specific surface area, ion-exchange capacity, and pozzolanic reactivity [16]. Porous materials such as zeolite, fly ash, silica fume, nano silica, metakaolin, slags, rice husk ash, corn cob ash, ternary geopolymer, and bagasse ash have been shown to replace cement partially or entirely in order to enhance the strength and durability of geopolymer-stabilized clays [26,27]. Compared to other supplementary cementitious materials (*SCM*), such as fly ash, silica fume, slag, and metakaolin, natural zeolite has its own set of qualities in terms of performance, pricing, and availability. Because industrial byproducts such as fly ash, slag, silica fume, and metakaolin rely on their local sources, they also require significant amounts of processing, which is different from the nature's own abundant resource that is natural zeolite, requiring only crushing and sieving, with up to 80 % less power requirements in comparison to cement [19]. Compared to other *SCM*s in terms of high pozzolanic activities and the formation of stable *C-S-H/C-A-H* gels with high long-term strengths, it is more durable [4]. Ni et al [28] showed that the combined use of lime and straw efficiently enhances the strength and durability of stabilized dredged sludge. Wang et al [29] demonstrated that fly ash-based ternary alkali-activated materials, combined with slag and desulfurization gypsum, effectively improve the strength and durability of dredged sediments. Among these replacement materials, Zeolite has been reported to result in an environmentally friendly and low-cost alternative with high adsorption and ion exchange properties due to its crystalline structure [30,31]. Zeolite can be grouped into two main categories: natural zeolites such as clinoptilolite, mordenite, and garronite; and synthetic zeolites such as zeolite A, P, X, and Y [32]. Natural zeolites are commonly used to adsorb hazardous contaminants like heavy metals. Zeolite exhibits a particularly high adsorption capacity, reaching approximately 40 % of its own weight [33].

A study of high plasticity clays stabilized with zeolite in landfill liners using wet-dry (*W-D*) cycles revealed that shrinkage and swelling were significantly reduced [34]. Sharo et al [35] conducted a series of mechanical tests to investigate the effects of natural zeolite in combination with cement kiln dust on high-plasticity clay. Furthermore, the addition of natural zeolite (due to its pozzolanic activity) enhanced the workability, strength, durability, and permeability [36]. The calcium hydroxide produced by cement hydration reacts with silicon dioxide and aluminum oxide to form calcium silicate hydrate (*C-S-H*) and calcium aluminate hydrate (*C-A-H*) gels [37]. In general, the inclusion of cement in soil mixtures, even at minor proportions, can significantly affect the strength, and brittleness of cemented clays [38]. Such improvement depends on the properties of the parent clayey soil, initial void ratio or porosity of the soil, cement and water contents, as well as curing time, temperature, and the possible exposure to freeze-thaw (*F-T*) and *W-D* cycles [39–41].

The use of zeolite is particularly attractive as an alternative stabilizer because of its environmentally friendly nature compared to other supplementary cementitious materials [19]. Previous studies have demonstrated that zeolite can enhance mechanical performance by producing additional *C–S–H* gels and refining pore structure. For example, MolaAbasi et al [16] and Khajeh et al [42] reported that a 30 % replacement of cement by zeolite provided optimum strength and stiffness for stabilized sands and silty soils. Specifically, zeolite may prove to be a more economical alternative to cement due to its abundance and availability [43]. Also, the zeolite's crystalline structure, and high specific surface area, make it an ideal material to facilitate cation exchange [44]. Following a comparatively straightforward mining process, processing of natural zeolite typically involves few stages due to its fragile structure [45]. Zeolite powder is generally obtained by crushing the mined raw materials, grinding and sieving. Overall, zeolite production consumes significantly less energy compared to that required for cement manufacturing's multiple stages, resulting in fewer emissions of greenhouse gases [46,47]. Shahmansouri et al [48] investigated the use of natural zeolite as a supplementary cementitious material and reported that its incorporation improved the compressive strength and microstructural density of the blended mixtures while significantly reducing carbon emissions. As a result, from a sustainability perspective, zeolite utilization may be considered a attractive alternative to conventional cementitious materials. Recent life cycle assessment studies have also disclosed a 50–62 % *GHG* emission reduction, in addition to 54 % savings in costs, for partial substitution with zeolite or other pozzolanic materials in soil stabilization [4]. The results re-emphasize that the substitution with zeolite could be an economically viable strategy for mitigating *GHG* emissions in massive infra-structure construction for road stabilization work.

Several studies have been conducted on the geotechnical behavior of soils treated with zeolite. Findings from Osman and Al-Tabbaa [49] indicate that clays stabilized with mixtures of cement and zeolite performed better, in terms of unconfined compressive strength (*UCS*) and *F-T* performance, than those stabilized solely with cement. Shi [50]

reported that partial replacement of cement with zeolite results in improved treatment effectiveness across a range of soils, from coarse- to fine-grained soils, as the curing time increases. The addition of both cement and zeolite to clay led to an increase in strength and reduction in swelling and dispersivity potential [51,52]. Using a 30 % replacement of zeolite, Chenarboni et al [13] showed that the amount of SiO_2 and Al_2O_3 (derived from the zeolite) is close to the amount of *CaO* (derived from the cement), which indicates an 30 % optimum value for the pozzolanic reactions used. Also, they reported that zeolite-cement-treated high plasticity clay resulted in increased maximum density and optimum moisture content with increasing zeolite content. Akbari et al [53] evaluated polypropylene fiber reinforcement of lime-nanozeolite-treated clay at 20 and 40 °C. As reported in this study, a 40 % lime replacement with nanozeolite (in an originally 10 % lime-treated clay) resulted in 20 and 7 times higher *UCS*, after curing for 28 days at 20 and 40 °C, respectively.

The study of cement-zeolite-treated clays has generally focused on their improved mechanical properties (e.g., *UCS*), with little emphasis on their durability and compressibility properties. MolaAbasi et al [16] investigated the durability and microstructure of cement-zeolite-treated sands. In general, the durability of the samples, as measured by accumulated loss of mass (*ALM*), increased with the addition of cement and decreased when the samples were subjected to *W-D* cycles [54].

The ultrasonic pulse velocity (*UPV*) testing method has been used in several studies to evaluate the engineering properties of geotechnical materials [55]. In this process, an electrodynamic pulse is applied to the surface of a solid, causing stress waves to propagate through its texture. The velocity of the stress wave is influenced by several parameters such as the density, structure and Poisson's ratio [56]. Therefore, it is possible to estimate various mechanical characteristics by quantifying the velocity of the passing compressional stress wave [57–59]. As the ultrasonic pressure wave velocity (V_P) can be correlated with the *UCS*, it is possible to continuously evaluate the effect of additives on soil strength and durability by using a comparatively limited number of specimens [60,61]. Based on *UPV* test results, the V_P and constrained modulus (*CM*) can be calculated as representative stiffness parameters [62]. Su et al [62] evaluated the effect of *F-T* cycles on the *CM* and *UCS* of various soils (clay, silt, sand, and gravel) that had been treated with cement, lime, and fly ash. The results of the study indicated that *F-T* cycles significantly reduced the *CM* and *UCS* of the treated specimens. Yet, the influence of *F-T* cycles was meaningfully reduced by increasing fly ash additive content. In similar research, Mandal et al [63] investigated the dynamic response of cement-, lime- and fly ash-improved soil and found that the inclusion of additives increased both V_P and *CM*. Furthermore, correlations were developed between flexural strength and *CM*. According to Biswal et al [64], *UPV* tests was successful to assess the strength and stiffness of cement-stabilized granular lateritic soils, and a higher cement content improved V_P. Based on the *UPV* test results, correlations for estimating compressive, flexural and indirect tensile strengths were proposed [64]. A power relationship was developed to relate the *UCS* and V_P in cement- and zeolite-stabilized high plasticity clays [4]. Finally, Subramanian et al. [65] investigated the stiffness properties of cement-treated clay in *UPV* tests and found that adding sand to cement-treated clay improved its *CM*.

Life cycle assessment (*LCA*) and life cycle cost (*LCC*) are well-established methods for investigating potential sustainability effects and economic costs associated with project life cycle phases, including construction, maintenance, use and end-of-life phases [66,67]. In *LCA*, resource consumption, emissions and ecological effects are assessed at every stage of the given process to ensure sustainability and reduce costs [68,69]. By incorporating factors such as raw material costs, operating costs and end-of-life expenses, *LCC* provides a comprehensive economic analysis to assist indecision-making [70].

The review of studies on clay stabilization using zeolite showed improvements in soil strength, durability, and sustainability. However, there is a significant research gap related to the application of *UPV* testing to the examination of the Durability and compressibility of stabilized high plasticity soils. The purpose of the present study was to investigate the variation in *ALM*, V_P and *CM* in high-plasticity clays treated with various amounts of cement and zeolite after 56 days of curing. In addition, and in order to further assess the implications of adopting an optimal zeolite and cement contents, an *LCA* and *LCC* were conducted based on *UPV* test results. This paper addresses road construction specifically, where maximizing the durability and sustainability of subgrade soils is crucial to long-term pavement durability and cost savings.

2. Materials and methods

2.1. Materials

In this study, high plasticity clay samples were collected in Mahshahr, Khouzestan province, Iran. As illustrated in Table 1, the physical properties of the high plasticity clay were determined in accordance with ASTM standards. Using the standard compaction test (ASTM D698), the optimum moisture content (*OMC*) and maximum dry unit weight (*MDUW*) were determined to be 22 % and 15.4 kN/m^3, respectively. The specific gravity (G_s) of the soils was 2.68 (ASTM D854). According to ASTM D4318, the liquid limit (w_L) and plasticity index (*PI*) were 73 % and 29 %, respectively. The soil is classified as clay with high plasticity (*CH*) according to the Unified Soil Classification System (*USCS*) (ASTM D2487).

Portland cement type *II*, with a G_s of 3.11, was used as the main stabilizer. In partial replacement of cement, a clinoptilolite-type natural zeolite was used as an additional stabilizer. Cement Type *II*, widely employed in Iran, was utilized because of its compatibility with zeolite. Clinoptilolite-type zeolite was utilized due to its excellent pozzolanic activity and ability to react with cement hydration products to enhance the strength and durability of expansive soils [46,71]. The zeolite is a low-plasticity silt-sized powder that classifies as *ML* according to the *USCS*, with a specific gravity of 2.18. In addition, Fig. 1 presents the particle size distribution of both stabilizers and the high-plasticity clay.

Fig. 2 illustrates the results of X-ray fluorescence (*XRF*) tests performed on high plasticity soil, cement, and zeolite. According to the *XRF* test results, *CaO* was established as the major component of the cement. Two oxides, SiO_2 and Al_2O_3, were primarily present in the zeolite at concentrations that, when combined, exceed 70 %, which meets the requirements of ASTM C618 to classify as a pozzolanic material. According to Chenarboni et al [13], the SiO_2 and Al_2O_3 present in the high-plasticity clay have no significant effect on the reactions triggered by cement and zeolite.

2.2. Sample preparation

To determine the effect of cement and zeolite on the engineering behavior of high plasticity clay, 24 clay specimens were cast in cylindrical *PVC* molds with a height-to-diameter ratio of approximately 2

Table 1
Physical properties of the high-plasticity clay evaluated in this study.

Properties	Value
Specific gravity, G_s	2.68
Atterberg limits (%)	
Liquid limit, w_L	73
Plastic Index, *PI*	44
Grain-size distribution (%)	
Sand	4
Silt	60
Clay	36
Compaction characteristics	
Maximum dry unit weight, (kN/m^3)	15.4
Optimum moisture content, (%)	22.0
Unified Soil Classification System	CH

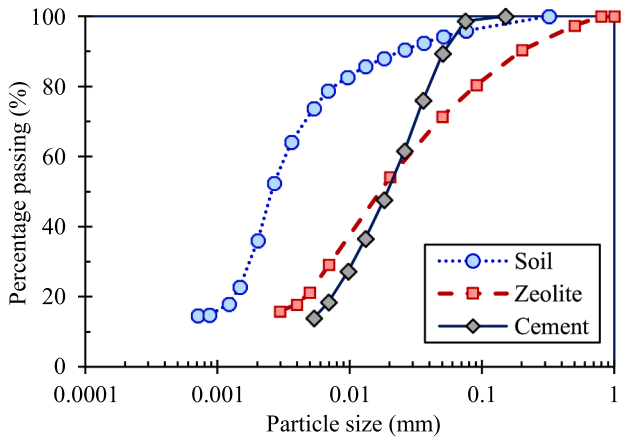

Fig. 1. Particle size distribution curve of soil from Mahshahr city, zeolite, and cement used in this study.

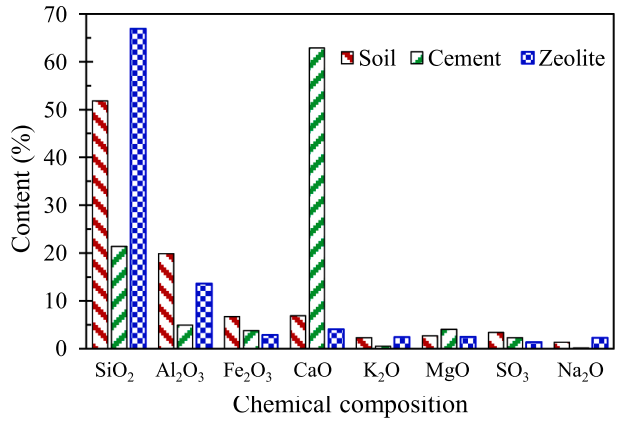

Fig. 2. Chemical composition of the high-plasticity clay, cement, and zeolite.

(100 mm in height to 50 mm in diameter). After preparing the soil stabilized mixtures, each specimen was compacted in five layers inside the mold to achieve initial conditions defined by the *MDUW* and *OMC* parameters, as obtained from compaction test results performed in similar studies [13]. All the specimens were statically compacted to reach the target dry density in order to prepare uniform specimens. To ensure proper interconnection between layers, the top of each layer was scarified. For effective bonding of the layers, the surface of each compacted layer was scarified to a depth of approximately 2 mm before adding on the next layer. All test specimens were cured for 56 days at 23 ± 2 °C temperature and humidity above 95 %, according to ASTM D1632. Stabilizers at total concentrations S of 6 %, 8 %, 10 %, and 12 % were added to the clay specimens. Cement is considered the base stabilizer, whereas zeolite was used as the replacement stabilizer. For each one of the four stabilizer concentrations, zeolite was used at replacement ratios Z of 0 %, 10 %, 30 %, 50 %, 70 %, and 90 %, selected based on preliminary laboratory experiments and supported by previous studies [4,13]. The specimens were subjected to 12 sets of *W-D* cycles after a 56-day curing period. In accordance with ASTM D559, the specimens were first kept at 71 °C for 42 h and then at 23 °C in a water bath for another five hours. Views of the prepared specimens are shown in Fig. 3 at stages immediately after preparation, as well as after one and 12 cycles of *W-D*. The samples were weighed and *UPV* tests were performed. After each *W-D* cycle, the *ALM* of the samples was calculated to quantify the durability of the specimens. The *ALM* is a measure of the specimen durability, determined as the percentage change in weight after *W-D* cycles in relation to the initial specimen weight.

2.3. UPV test procedures

The *UPV* test is a non-destructive evaluation method that has been widely adopted in previous research involving the characterization of concrete. In geotechnical engineering, the results of *UPV* testing can be used to determine whether cementitious additives are suitable to stabilize soil samples. Following specimen curing, the effect of stabilizer content and zeolite replacement on V_P values was determined utilizing a Proceq Punditlab *UPV* device. Fig. 4 displays the *UPV* device used in this study, which consists of a central unit that generates signals and two P-wave transducers that transmit and receive the signals. To measure V_P, the 50-mm-diameter transducers provided a transmission frequency of 54 kHz and an amplitude of 500 V. To minimize the presence of air or voids between the specimen surfaces and transducers, the specimen surfaces were covered with coupling gel during testing. The device measured a pulse transmission time (T) with a precision of 0.1 s with the transmission length (L) being defined according to the specimen height. The V_P could then be directly calculated as:

$$Vp = \frac{L}{T} \tag{1}$$

Using the measured V_P for the specific curing time and ρ for bulk density of the specimen, the *CM* of the specimens was then calculated as follows:

$$CM = \rho(V_P)^2 \tag{2}$$

2.4. Sustainability and economic assessment

Evaluation of the carbon footprint associated with different human activities and processes has become increasingly important as it corresponds to one of the indicators that can be quantified to evaluate global warming. Further, it is essential that carbon emissions are measured and reduced [68]. To assess the sustainability and economic effects of using zeolite in road construction, *LCA* and *LCC* were quantified for a representative roadway project. The research framework for *LCA* and *LCC* comprises four stages: (1) defining the research goal; (2) conducting an inventory analysis; (3) performing an impact assessment; and (4) interpreting the results [72]. The *LCC* analysis is similar to *LCA*, with the key difference being that *LCC* focuses on calculating costs rather than carbon emissions [73,74].

The goal of the evaluation conducted in this study is to evaluate the amount of carbon emissions produced during road construction and explore potential methods for reducing these emissions. Consequently, this study is limited to the cradle-to-site stages. Fig. 5 presents a schematic of the carbon emission factors associated with road construction. As indicated in Fig. 5, the functional unit was defined as a road section measuring 1000 m in length, 6 m in width and 0.3 m in height. The primary sources of carbon emissions include raw materials (e.g., cement, zeolite, water) as well as energy consumption from construction equipment. Therefore, the inventory analysis in this study involves collecting and calculating carbon emissions from raw materials, transportation, and energy consumption of construction equipment. Table 2 provides detailed information on the carbon emission factors and cost units related to raw materials, energy consumption, and transportation. The primary goal of the assessment was to evaluate relative environmental and economic trends associated with incremental zeolite substitution under consistent project assumptions.

At the impact assessment stage, the carbon emissions generated during road construction were calculated using the inventory data, including the quantities of materials and energy consumed. In the final stage, the results of the carbon emissions were interpreted, and the evaluated emissions were used to develop strategies for reducing carbon emissions as much as possible. A formal sensitivity analysis was not conducted because the scope of the research in the original investigation focused on trend identification instead of optimization processes. All

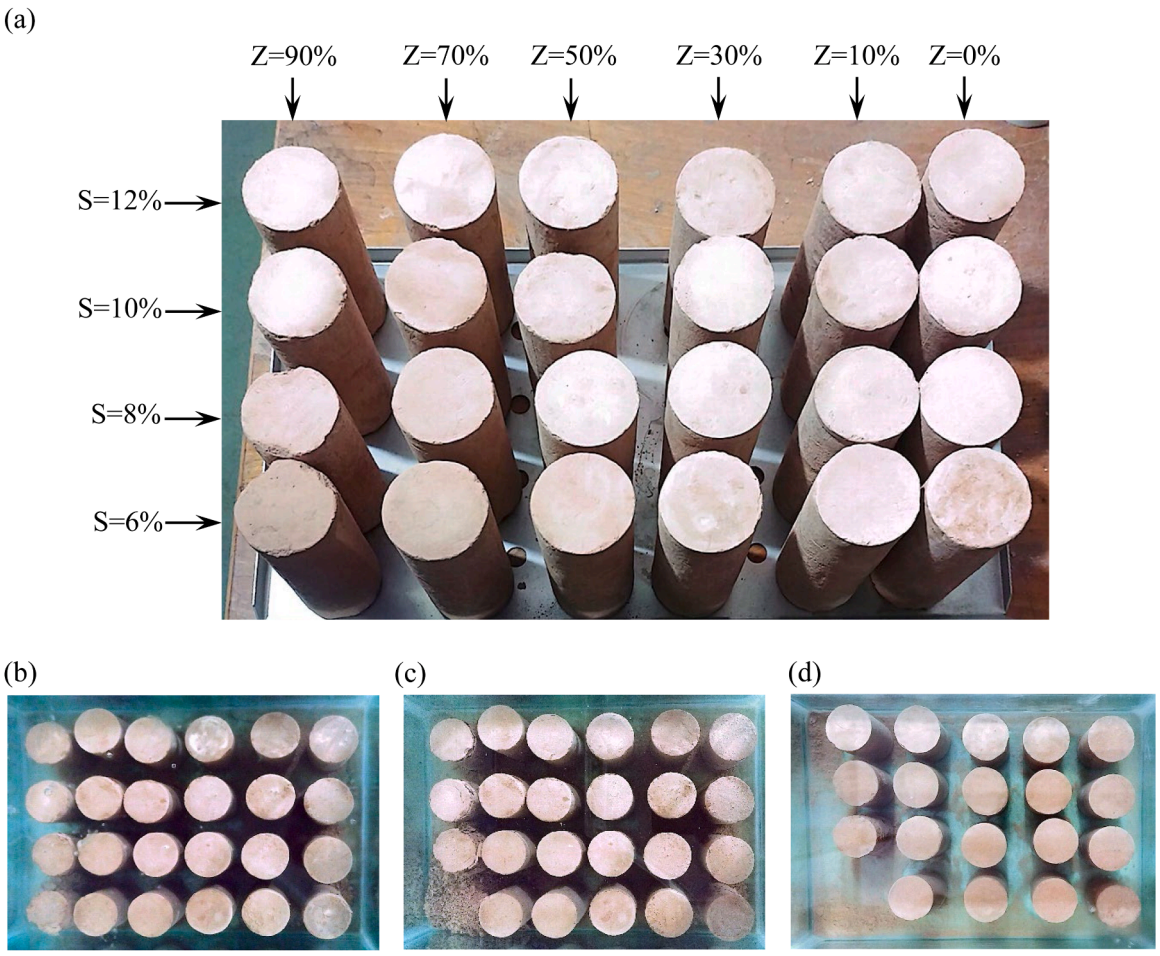

Fig. 3. View of the speciens prepared with four stabilizer contents ($S = 6$ %, 8 %, 10 %, and 12 %) and six zeolite replacement ratios ($Z = 0$ %, 10 %, 30 %, 50 %, 70 %, and 90 %): (a) specimens after preparation; (b) specimens during initial wetting cycle; (c) specimens after first drying cycle; and (d) specimens after 12 cycles.

Fig. 4. *UPV* testing device and view of specimen during testing.

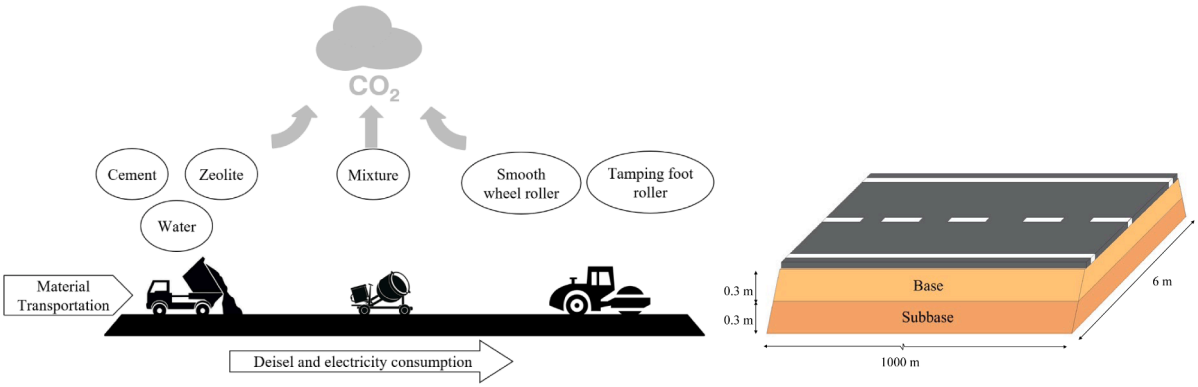

Fig. 5. Calculation boundary of carbon emissions cradle to a road construction site and functional unit of base and subbase for cement-zeolite stabilizer.

Table 2
Carbon emission factors and costs of raw materials, fuel, transportation, and composite materials.

Item		Carbon emission factor (kg CO_2-eq/ Unit)	Cost (USD/ Unit)	Reference
Material	Cement: t	900	110.2	Yuan et al [75]; Ghayeb et al [76]
	Water: m^3	0.41	0.88	Mao et al [77]; Tang et al [78]
	Zeolite: t	1.41	37	MolaAbasi et al [54]
Fuel	Diesel: kg	4.16	1.04	Yuan et al [75]; Zhang et al [74]
Transportation	Truck: 1/t. km	0.18	0.67	MolaAbasi et al [54] MolaAbasi et al [54]
Construction machines	Smooth wheel roller: L/h	0.42	3.7	
	Tamping foot roller: L/h	0.67	5.92	

scenarios were modeled using fixed boundary conditions in order to make comparisons between mixtures with equivalent criteria. Future research should also incorporate uncertainty analyses for validating the sensitivities in the outcomes obtained for *LCA* and *LCC* results.

3. Results and discussion

3.1. Effect of W-D cycles and zeolite content on ALM

Several parameters can be considered to quantify the durability of stabilized specimens. The *ALM* is among the most suitable parameters to determine the durability of specimens subjected to *W-D* cycles and evaluate their durability characteristics. The *ALM* reveals changes in the sample weight during *W-D* cycles. The higher cement content helps in improving the bonding between particles, in addition to encouraging a more comprehensive hydration reaction, leading to the formation of denser *C-S-H/C-A-H* gels with reduced connectivity that resists water diffusivity. As a result, the samples with higher cement content show reduced weight loss during the cycles of *W-D* tests. As these samples undergo continuous cycles of *W-T* treatments, the hydration bonds get compromised due to micro-cracking, dissolution of calcium hydroxide, and shrinkage forces in samples with insufficient binder content [79]. Since an increase in cement content strengthens the bonding between particles, durability and weight are expected to decrease during *W-D* cycles. For stabilizer contents of 6 %, 8 %, 10 % and 12 %, the results in Fig. 6 show the changes in *ALM* with increasing number of *W-D* cycles and for different zeolite replacement ratios. Every subfigure in Fig. 6 is assigned the notation of S6, S8, S10, and S12, respectively, representing stabilizer contents of 6 %, 8 %, 10 %, and 12 %. As the number of *W-D* cycles increased, the *ALM* was observed to increase as a result of the specimen bond destruction. In 90 % zeolite replacement specimens, the number of *W-D* cycles to the complete destruction of specimens was one, three, five, and six for 6 %, 8 %, 10 %, and 12 % stabilizer content, respectively. Further, the specimens with 70 % zeolite replacement containing 6 % stabilizer content brought about the complete destruction of specimens after 6 W-*D* cycles. Beyond the last marked point, the samples were completely destroyed, and the *ALM* was 100 %, indicating complete destruction.

As a result of the pozzolanic reactions and hydration process, increasing the stabilizer content was found to decrease the *ALM*. Furthermore, the *ALM* was also found to decrease with increasing zeolite replacement ratio of up to a value of 30 %, with the *ALM* starting to increase with continued increase in the zeolite replacement ratio beyond 30 %. Accordingly, the results of this evaluation indicate that a zeolite replacement ratio of 30 % resulted in an optimum value that led to a minimum *ALM* value, independent of the actual stabilizer content. The reduction in *ALM* that can be observed at up to 30 % zeolite contents can be attributed to the enhanced pozzolanic activity of zeolite, which interacts with calcium hydroxide ($Ca(OH)_2$) released due to hydration of cement and forms more of the calcium silicate hydrate (*C–S–H*) and calcium aluminosilicate hydrate (*C–A–S–H*) gels. The reaction products fill the microstructure, fill pore space, and strengthen the interfacial bond between particles of the soil and hence reduce the loss of mass during *W-T* cycles. With higher zeolite contents, the reduction in available $Ca(OH)_2$ limits the formation of *C–S–H* and *C–A–S–H* gels, leading to incomplete pozzolanic reactions and weaker particle bonding beyond the 30 % replacement level [16]. The stabilized soil is susceptible to erosion and detachment of particles, that is, an enhancement with *ALM* at high levels of zeolite.

3.2. Effect of W-D cycles and zeolite content on V_P and M

Fig. 7 shows the V_P results obtained for soil specimens stabilized with cement and zeolite and subjected to an increasing number of *W-D* cycles. As expected, increased stabilizer contents lead to specimens with higher V_P values due to the increased number of hydration products forming strong bonds with the clay particles. The optimum zeolite replacement ratio (Z_{opt}) Was observed to be 30 %, which, in turn, led to the highest V_P values of 1680, 1879, 2068, and 2249 m/s for stabilizer contents of 6, 8, 10, and 12 %, respectively. Hence, the results indicated that the specimens with a 30 % zeolite replacement ratio resulted in the highest V_P, which is consistent with the optimum replacement ratio obtained from evaluation of the *ALM* test results. These findings are consistent with the results reported by MolaAbasi et al [37], who indicated that an optimum

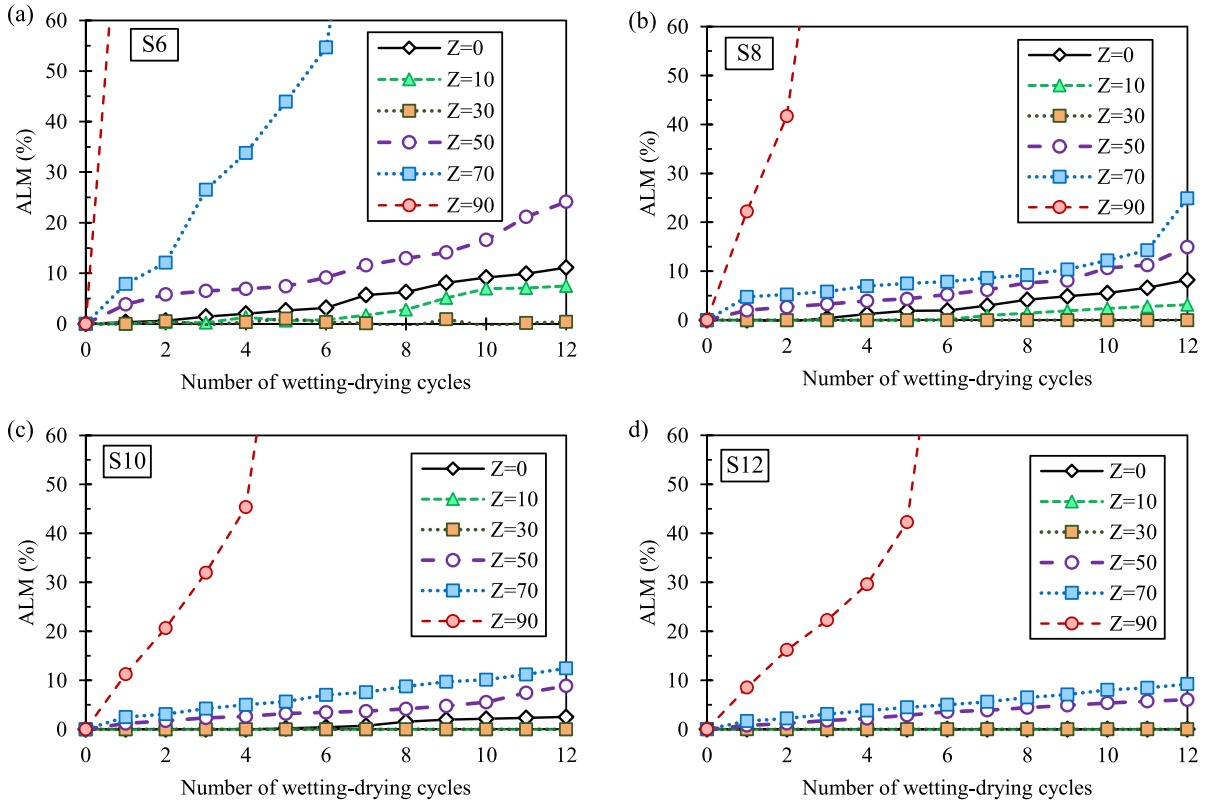

Fig. 6. Changes in *ALM* with increasing number of *W-D* cycles (and for zeolite replacement ratios ranging from 0 to 90 %), for the different stabilizer contents evaluated in this study: a) 6 %; b) 8 %; c) 10 %; and d) 12 %.

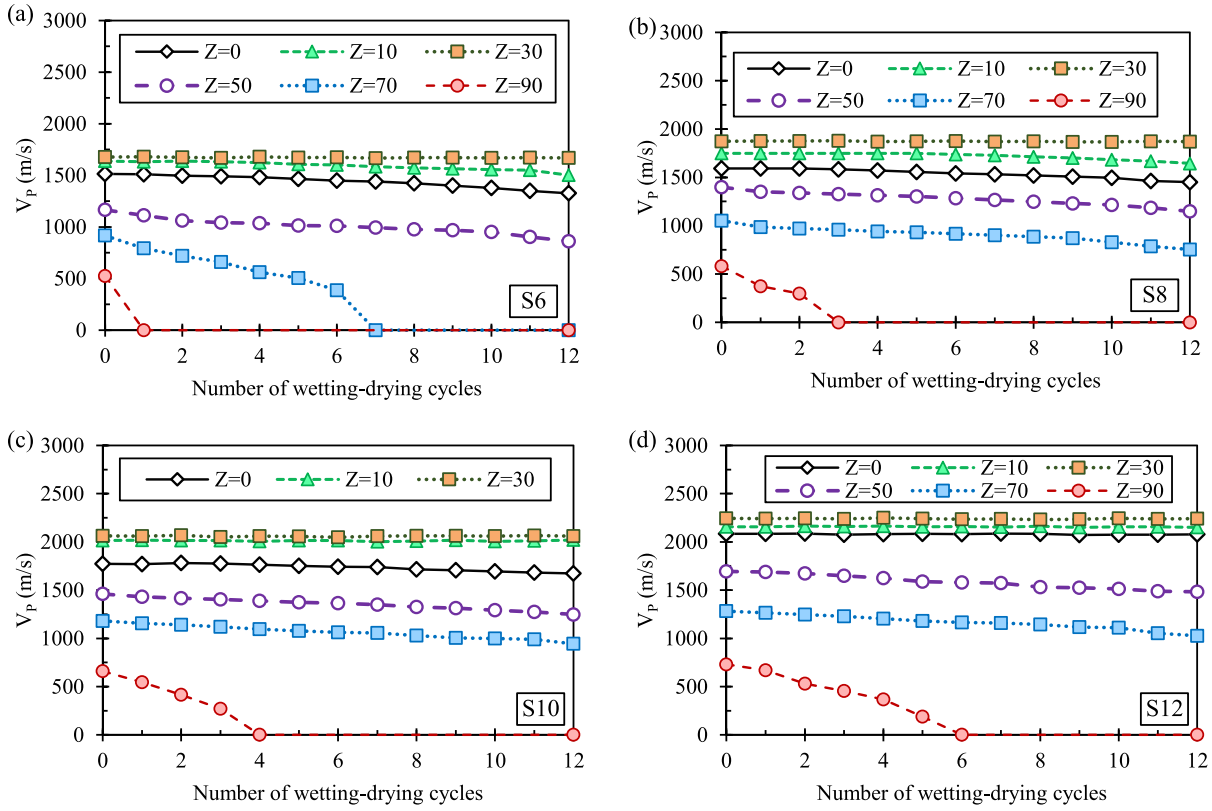

Fig. 7. Influence of number of *W-D* cycles and zeolite contents on V_P for stabilizer contents of: a) 6 %; b) 8 %; c) 10 %; and d) 12 %.

replacement ratio of 30 % may be related to pozzolanic reactions with $Ca(OH)_2$ in cement, and SiO_2 and Al_2O_3 in zeolite, leading to major hydration products like *C-S-H*. The optimum V_P value observed at a zeolite replacement level of 30 % can be attributed to the perfect balance between cement hydration and pozzolanic reaction of zeolite. At the replacement level, zeolite intensely reacts with the calcium hydroxide ($Ca(OH)_2$) formed during cement hydration to form more calcium silicate hydrate (*C–S–H*) and calcium aluminosilicate hydrate (*C–A–S–H*) gels. The gels occupy the micro voids, densify interparticle bonds, and form a denser and rigid structure that increases V_P. When >30 % of zeolite content is present, the amount of available Ca^{2+} ions for activation of the pozzolanic reaction is not enough to yield full gelation. The excess zeolite particles remain as unreacted inclusions that disrupt the continuity of the cementitious matrix. This reduces the network stiffness and homogeneity and leads to lower V_P values. Thus, the best 30 % zeolite replacement is that where microstructural densification and strengthening are improved.

All the specimens exhibited a reduction in V_P as *W–D* cycles were increased, which was uniform at about 30 % zeolite replacement. Wetting in each cycle causes swelling due to water adsorption and pore expansion, and drying produces shrinkage due to the creation of micro- and macrocracks within the cementitious matrix. These fractures disrupt the solidity of the skeleton continuity and reduce stress-wave transmission efficiency, thus resulting in lowering V_P values. Throughout repeated cycles, crack opening and closure continually further degrade particle bonds and increase physical deterioration, creating cumulative stiffness loss and scaling of specimen surfaces [80].

Fig. 8 shows the effect of stabilizer content and zeolite replacement ratios on the *CM* of specimens that were subjected to 0, 5 and 12 W-*D* cycles. The results show that the *CM* increased with an increase in stabilizer content. The optimum ratio of zeolite replacement was 30 %, which led to an increase in *CM* values. Consequently, the results indicated that the sample consisting of >30 % zeolite replacement had an increased constrained modulus, confirming the V_P and *ALM* results.

For a zeolite replacement ratio of 0 %, the results in Fig. 8 indicate that, as expected, the constrained modulus increases with increasing stabilizer content. However, such an increase is compromised by the number of *W-D* cycles, with an increase in stabilizer content from 6 to 12 % resulting in an increase in constrained modulus of 97 % before *W-D* cycles to an increase of 155 % after 12 W-*D* cycles. This indicates that specimens with lower stabilizer contents are more sensitive to *W-D* cycles and specimens with higher stabilizer contents are more durable. On the other hand, for a zeolite replacement ratio of 30 %, the results in Fig. 8 indicate that the increase in constrained modulus with increasing stabilizer content is essentially independent of the number of *W-D* cycles. Specifically, an increase in stabilizer content from 6 to 12 % resulted in an increase in constrained modulus of about 88 %, independent of the number of *W-D* cycles.

Table 3 indicates the mean, standard deviation, and coefficient of variation (*CV*) of V_P in three replicate specimens with 30 % zeolite replacement (*Z30*) and different contents of stabilizer (*S6, S8, S10*, and *S12*) under different *W-D* cycles. Low standard deviation and *CV* values indicate high reliability and repeatability of the V_P measurements. For the *ALM*, no measurable weight loss was recorded in all replicates, thereby confirming the hardness and stability of the specimens at test conditions.

3.3. Optimization of the zeolite replacement ratio

Fig. 9 shows the changes in V_P with increasing zeolite replacement ratio for the four different stabilizer contents adopted in this study. The optimum zeolite content of approximately 30 % is the outcome of the equilibrium between available calcium from cement hydration and zeolitic pozzolanic activity. At this content, the formation of additional *C–S–H* and *C–A–S–H* gels densifies the microstructure and enhances durability. Beyond 30 %, calcium depletion limits the gel formation,

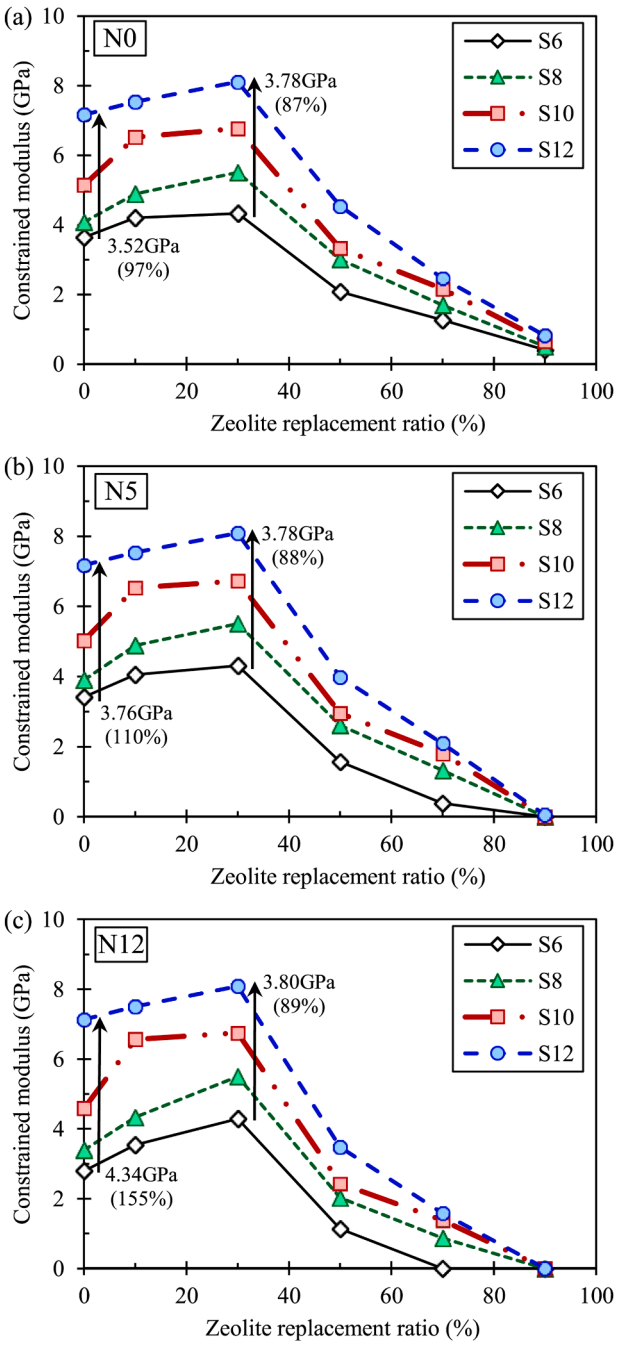

Fig. 8. Comparison of constrained modulus for increasing zeolite contents at different stabilizer contents after: a) 0; b) 5; and c) 12 W-D cycles.

while the remaining unreacted zeolite has the tendency to impair the matrix continuity and reduce V_P and strength, in agreement with past research [13,31]. It is notable that, as previously discussed, not only are the durability and constrained modulus the highest for a 30 % zeolite replacement ratio (see Figs. 6, 7 and 8), but as shown in Fig. 9, the effect of increasing the number of *W-D* cycles is negligible. Specifically, the *W-D* cycles resulted in a V_P reduction of only 0.5 % at a 6 % stabilizer content, with such a reduction being even lower (0.1 %) for higher stabilizer contents (8 %, 10 %, and 12 %). As a reference, it should be pointed out that in specimens without zeolite, an increase in stabilizer content from 6 % to 12 % resulted in a V_P reduction due to *W-D* cycles from 12.4 % to 0.2 %.

As shown in Fig. 9a for specimens with a 6 % stabilizer content, the

Table 3
Statistical summary of pressure wave velocity results for specimens with 30 % zeolite replacement (Z30) and different stabilizer contents (S6, S8, S10, and S12) under varying numbers of W–D cycles.

	Number of W-D cycles	Average (m/s)	Standard deviation (m/s)	coefficient of variation (%)
S6	0	1676	4.15	0.25
	5	1672	4.75	0.28
	12	1668	5.28	0.32
S8	0	1873	4.32	0.23
	5	1873	5.10	0.27
	12	1871	3.86	0.21
S10	0	2063	3.45	0.17
	5	2057	2.96	0.14
	12	2060	3.26	0.16
S12	0	2244	2.54	0.11
	5	2241	2.91	0.13
	12	2241	2.56	0.11

effect of *W-D* cycles on V_P was significant for specimens with 0 % zeolite, decreased to under 10 % with the addition of 5.8 % zeolite, and reached its minimum at 30 % zeolite replacement ratio. A continued increase in the zeolite replacement ratio resulted in an increase in the effect of *W-D* cycles, which exceeded 10 % in specimens with a zeolite replacement ratio of 37.5 %. Conversely, as shown in Figs. 9b–9d, specimens with high stabilizer contents showed improved durability for a 0 % zeolite replacement ratio, with the effect of *W-D* cycles remaining below 10 % and decreasing with increasing stabilizer content, with the lowest effect of *W-D* cycles observed at a 30 % zeolite replacement ratio. The maximum zeolite replacement ratios that would still keep the effect of *W-D* cycles below a maximum acceptable value of 10 % for stabilizer contents of 6 %, 8 %, 10 % and 12 % were 37.5 %, 41.1 %, 43.7 % and 46.0 %, respectively.

As shown in Fig. 9, the velocity of pressure waves *Vp* increases with increasing zeolite replacement ratio up to an optimum zeolite ratio of 30 %, whereas the velocity decreases with increasing zeolite ratio beyond this value. Accordingly, the *Vp* trends reach a peak pressure wave velocity (V_{Pmax}) for the optimum zeolite content (Z_{opt}). Similarly, the V_P of the specimen with a reference zeolite replacement ratio (Z_r) is equal to the V_P of the specimen without zeolite. Amounts of Z_r at different *W-D* cycles and stabilizer contents are shown in Fig. 9. When *W-D* cycles are increased for each stabilizer amount, Z_r content remains approximately constant.

Fig. 10 shows the predicted reference zeolite replacement ratio obtained for increasing number of *W-D* cycles and for the various stabilizer contents adopted in this study. The fitting of the evolution of the Z_r with the number of *W-D* cycles was estimated by the root mean square error (*RMSE*) and coefficient of variation (*CV*). The calculated RMSE values were 0.936, 0.396, 0.405, and 0.676, and the corresponding *CV* values were 2.79 %, 1.05 %, 1.13 %, and 2.11 % for S6, S8, S10, and S12, respectively. Lower *CV* and *RMSE* values obtained for S8 and S10 also indicate that Z_r was less fluctuating in the repeated *W-T* cycle, validating the better stability and reproducibility of the latter mixtures. As S8 and S10 denote mixtures with greater Z_r values, the trend here suggests that higher zeolite content can effectively replace cement without exhibiting hugely different mechanical and durability properties. That is, the low *RMSE* and *CV* indicate that, at these stabilizer levels, Z_r is less sensitive to cyclic degradation, and the material system achieves a more stable response with increased zeolite substitution. According to the results presented in this figure, the specimen with 8 % stabilizer content resulted in the highest Z_r. As a result, at 8 % stabilizer content, the V_P remained essentially constant after adding a 41.2 % zeolite replacement ratio. On the other hand, for a 12 % stabilizer content, adopting a 35.1 % zeolite replacement ratio results in an essentially constant V_P. Based on this analysis, it can be concluded that the adoption of an 8 % stabilizer content can be led to a higher zeolite replacement ratio while maintaining an essentially unchanged V_P. At higher stabilizer contents, the

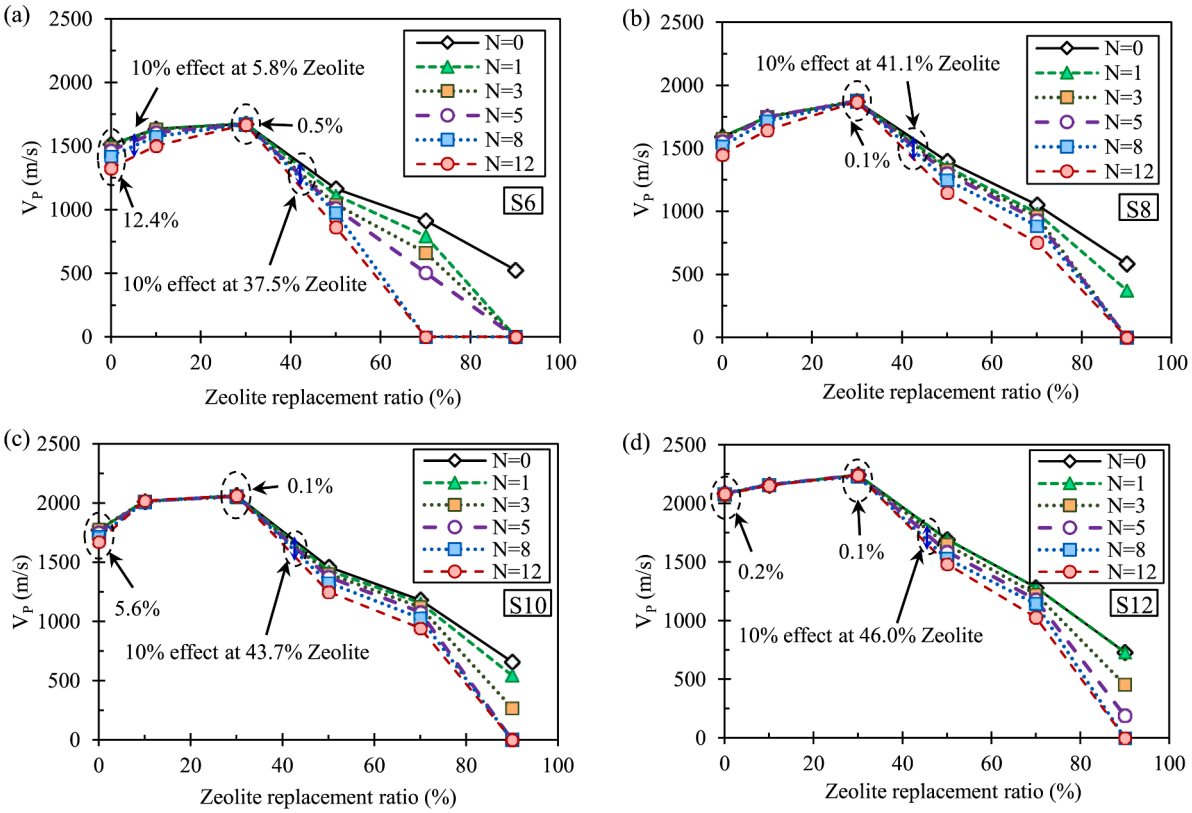

Fig. 9. Changes in V_P with increasing zeolite replacement ratio and increasing number of W-D cycles for stabilizer content values of: a) 6 %; b) 8 %; c) 10 %; and d) 12 %.

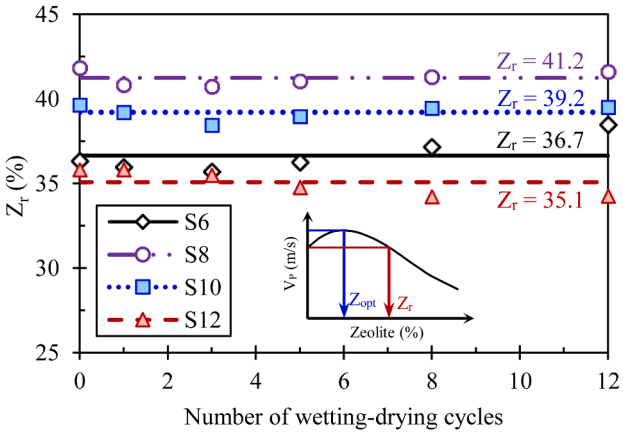

Fig. 10. Reference Zeolite replacement ratio for which the V_P is the same as that for 0 % zeolite replacement ratio.

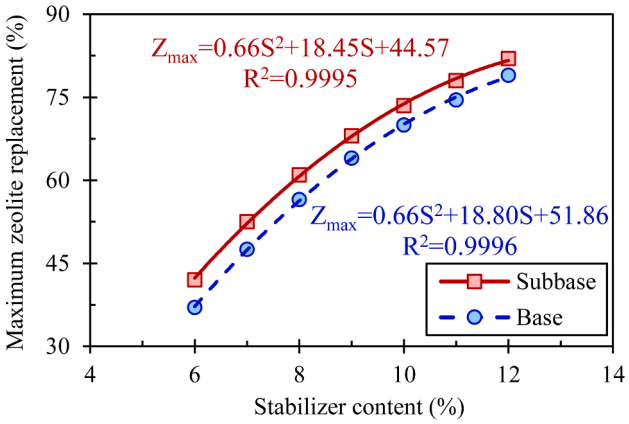

Fig. 11. Empirical relationship between maximum zeolite and stabilizer contents to obtain minimum *UCS* for road base and subbase construction.

superior performance of cement compared with zeolite can be attributed to both its finer particle size and faster hydration kinetics. The smaller cement particles provide a greater surface area and a higher number of nucleation sites for *C–S–H* formation, which accelerates early hydration and produces a denser, more cohesive matrix. In contrast, zeolite exhibits a lower intrinsic reactivity because its aluminosilicate structure is more crystalline and depends on the availability of $Ca(OH)_2$ released from cement hydration to initiate secondary pozzolanic reactions. When a large portion of cement is replaced by zeolite, the amount of available $Ca(OH)_2$ becomes insufficient, leaving part of the zeolite unreacted. This "calcium-limiting" condition, combined with zeolite's slower dissolution rate, leads to reduced formation of hydration products and higher residual porosity. Moreover, zeolite's angular morphology and internal porosity increase the water demand of the mix and disrupt the optimal packing density achieved by fine cement grains. Consequently, while moderate zeolite replacement (~30 %) enhances microfilling and long-term pozzolanic activity, excessive substitution dilutes the binder phase and weakens the inter-particle bonds. These coupled chemical ($Ca(OH)_2$ availability), kinetic (reaction rate), and physical (packing and pore refinement) mechanisms explain why finer cement performs better than zeolite at higher contents and why additional zeolite cannot effectively replace cement beyond the optimum ratio.

Several researchers have reported a direct relationship between *UCS* and V_P ([61]). MolaAbasi et al [4] presented the relationship between *UCS* and V_P for cement-zeolite-soil specimens as follows:

$$\text{UCS (kPa)} = 1203 V_P \left(\frac{km}{s}\right)^{1.995} \quad (3)$$

The minimum UCS of base and subbase materials is 1200 kPa and 1000 kPa, respectively (ASTM D1883). These thresholds correspond to the strength requirements for base and subbase layers in low- to medium-volume roadways, ensuring adequate bearing capacity and durability under repeated traffic loading, and are consistent with regional pavement design standards. Fig. 11 illustrates the relationship between the maximum zeolite and stabilizer contents required to achieve the minimum *UCS* for the construction of road bases and subbases. The regression fitting for maximum zeolite replacement vs stabilizer content was an excellent correlation, with values for R^2 equal to 0.9995 for the subbase and 0.9996 for the base layers. These very high values of R^2 confirm the accuracy of the proposed polynomial relationships and show that stabilizer content has a significant influence on controlling the maximum possible zeolite replacement in both pavement layers. Zeolite content in different stabilizer compositions was determined for base and subbase materials in this study. Increasing stabilizer contents to meet the minimum *UCS* for base and subbase materials allows for the use of more zeolite in specimens. Zeolite can be used in road construction to reduce CO_2 emissions while improving strength and durability.

3.4. Results of life cycle assessment and life cycle cost

Fig. 12 illustrates the carbon emissions and costs associated with varying zeolite content in different stabilizer compositions for a given functional unit which is defined as 1000 m long, 6 m wide, and 0.3 m high road sections. In conventional road construction, soil stabilization is usually achieved mechanically by rollers, which is often ineffective for expansive soils due to their high swell potential. Expansive soils are also technically infeasible and economically impractical to replace with non-expansive soils; hence, zeolite stabilization is a more feasible and eco-

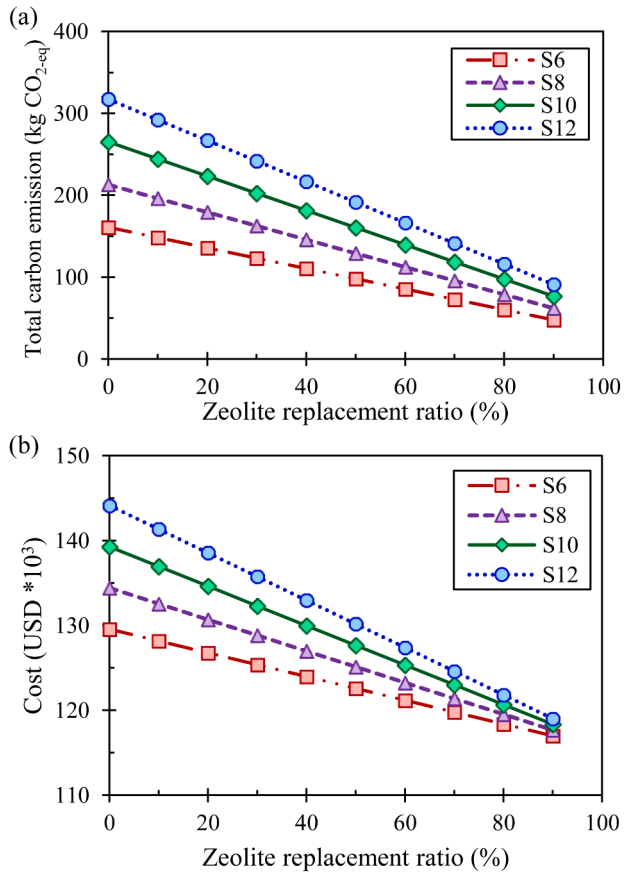

Fig. 12. Effect of zeolite replacement ratio for audits considering different stabilizer contents to quantify: a) total carbon emissions; and b) cost.

friendlier alternative. As is evident in the figure, increasing the zeolite replacement ratio resulted in a reduction in both carbon emissions and costs. For example, when considering S6 as a representative case, the carbon emissions decreased from 185,000 kg CO_2 at 0 % zeolite content to 70,000 kg CO_2 at 90 % zeolite content. This reduction is attributed to the substitution of zeolite for cement, as the carbon emissions from zeolite are significantly lower than those from cement. A similar trend can be observed in the cost analysis: given that zeolite is less expensive than cement, increasing the zeolite content led to a reduction in total costs, from $24,000 at 0 % zeolite to $11,000 at 90 % zeolite in the same case. Based on these results, zeolite can be considered a viable alternative to cement for reducing both costs and carbon dioxide emissions.

Fig. 13a depicts the carbon emissions related to the maximum zeolite and stabilizer contents necessary to meet the minimum *UCS* required for constructing road bases and subbases. The carbon emissions for both the base and subbase initially increased as the stabilizer content increased, eventually leveling off. As the stabilizer content grew, the percentage of zeolite replacement also rose, resulting in minimal changes in carbon emissions beyond a stabilizer content of 9 %. The carbon emissions from the base were lower than those from the subbase because the higher zeolite content in the base led to reduced overall carbon emissions. The implications for the construction of roads in a sustainable manner using these findings could be significant. They show that it is possible to reduce emissions (up to ≈ 60 %) and costs (up to ≈ 50 %) with a mix substituting cement partially with zeolite, yet meeting the mechanical criteria for pavement layers required in construction standards. Compared with traditional cement-stabilized layers in road construction, using zeolite in mixtures would result in layers with similar strengths but with much reduced emissions in line with the ever-growing need for sustainability principles in road construction technology today.

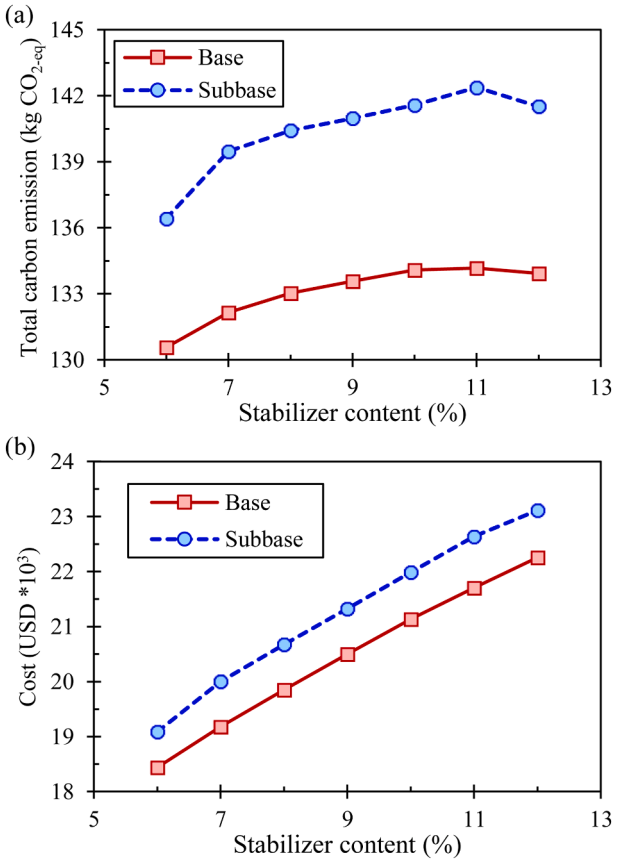

Fig. 13. Stabilizer contents at maximum zeolite for minimum required *UCS* in constructing road base and subbase layers: a) comparative carbon emissions; and b) cost analysis.

Fig. 13b shows the costs associated with the maximum zeolite and stabilizer contents needed to achieve the minimum *UCS* for road base and subbase construction. As the stabilizer content increased, construction costs also rose due to the increased consumption of materials such as cement. Consistent with the trend in carbon emissions, the costs for the base were lower than those for the subbase because of the higher zeolite percentage in the base.

4. Conclusions

This paper examines the simultaneous effects of using cement and zeolite to stabilize a high plasticity clay, with particular focus on the impact on V_P, constrained modulus and durability (*W-D* cycles). To determine the impact of adopting the optimum mixture, *LCA* and *LCC* evaluations were conducted using different amounts of cement to replace zeolite in base and subbase construction. The main findings of this study are as follows:

1 The results showed that zeolite replacement with cement below 30 % improved the durability and decreased *ALM* because it contains SiO_2 and Al_2O_3, which can produce pozzolanic reactions. Nonetheless, replacing more zeolite with cement causes a reverse effect, which results in destruction of the specimen in initial *W-D* cycles.
2 Specimens with low stabilizer contents were more sensitive to *W-D* processes, whereas specimens with higher stabilizer contents were more durable. However, specimens with 30 % zeolite replacement exhibited stable constrained modulus values across cycles, showing low sensitivity to stabilizer content changes. This suggests that while zeolite significantly enhances soil strength at lower stabilizer concentrations, its effect diminishes at higher stabilizer levels, particularly after 12 cycles of *W-D*.
3 A 30 % replacement of cement with zeolite was identified as the optimum ratio, resulting in the lowest accumulated loss of mass (*ALM*) and enhanced durability of the treated clay. In contrast, higher replacement levels (70–90 %) led to a decline in ultrasonic pulse velocity (V_P) and constrained modulus (*CM*), confirming that moderate zeolite substitution achieves the best balance between durability and mechanical performance.
4 Added zeolite enhanced V_P, peaking at 30 % replacement, where the effects of *W-D* cycles were negligible and durability increased. After 12 W-*D* cycles at 30 % replacement, V_P decreased by <0.5 %. Increasing the stabilizer from 6 % to 12 % without zeolite reduced the effect of *W-D* cycles from 12.4 % to 0.2 %. Overall, higher stabilizer content improved durability against *W-D* cycles, particularly at lower zeolite ratios. This suggests that zeolite is an important component of the stabilizer formulation. A low zeolite content in *W-D* cycles did not have a significant effect on V_P but adding more zeolite can increase the effect of *W-D* cycles, resulting in specimens of low strength and durability.
5 Increasing the zeolite replacement ratio in stabilizers leads to reduced carbon emissions and costs. For example, emissions decreased from 185,000 kg to 70,000 kg and costs fell from $24,000 to $11,000 as the zeolite content increased. In road construction, higher zeolite content reduces emissions and costs for the base and subbase, with emissions leveling off beyond 9 % stabilizer content. Overall, zeolite is demonstrated to be a sustainable and cost-effective alternative to cement for reducing environmental effects in construction projects.

Although this study comprehensively examined the durability and life-cycle performance of high-plasticity clays treated with zeolite as a partial cement replacement, several limitations should be acknowledged. First, the experimental program was limited to specific curing periods and environmental conditions, primarily *W-D* cycles, which may not fully represent the effects of other deterioration mechanisms such as

freeze–thaw action, sulfate attack, and long-term field weathering. Second, the life-cycle assessment was based on cradle-to-gate system boundaries and regional emission factors; therefore, extending the analysis to include transportation distances, maintenance scenarios, and end-of-life stages would provide a more complete sustainability profile. Third, the cost and social indicators were estimated using generic databases rather than region-specific data, which introduces some uncertainty in *LCA/LCC* comparisons. Future studies should include complementary durability tests (e.g., freeze–thaw, sulfate resistance, and chemical attack), large-scale field validation, and microstructural monitoring (e.g., *XRD* or *SEM* after durability tests). Expanding sustainability indicators, following frameworks such as Gao et al [15] and Strunge et al [19], will further enhance understanding of the long-term performance and circular-economy potential of zeolite-based soil stabilization.

CRediT authorship contribution statement

Pouya Alipanahi: Writing – original draft. **Paria Mirzaee:** Methodology, Investigation, Conceptualization. **Majid Naghdipour Mirsadeghi:** Writing – original draft, Formal analysis, Data curation, Conceptualization. **Farimah Fattahi Masrour:** Writing – original draft, Validation, Software, Resources, Conceptualization. **Farshad Yazdani:** Writing – original draft, Formal analysis. **Jorge G. Zornberg:** Writing – review & editing. **Hossein MolaAbasi:** Writing – review & editing, Project administration.

Declaration of competing interest

The authors declare that they have no known competing financial interests or personal relationships that could have appeared to influence the work reported in this paper.

Data availability

Data will be made available on request.

References

[1] M. Asadi, R. Mallick, S. Nazarian, Numerical modeling of post-flood water flow in pavement structures, Transp. Geotech. 27 (2021) 100468, https://doi.org/10.1016/j.trgeo.2020.100468.

[2] S. Banar, S.M. Haeri, A. Khosravi, M. Khosravi, Evaluation of strain-dependent shear modulus and damping ratio of unsaturated silty soil during drying path with resonant-column–torsional shear, In: Earthquake Geotechnical Engineering for Protection and Development of Environment and Constructions (2019) 1281–1288.

[3] N. Su, F. Xiao, J. Wang, S. Amirkhanian, Characterizations of base and subbase layers for mechanistic-empirical Pavement design, Constr. Build. Mater. 152 (2017) 731–745, https://doi.org/10.1016/j.conbuildmat.2017.07.060.

[4] H. MolaAbasi, O. Ataee, M.N. Mirsadeghi, F.F. Masrour, A. Marani, M.L. Nehdi, Investigation of high plasticity clay stabilized with cement and zeolite using time-dependent pressure wave velocity, J. Mater. Civ. Eng. 36 (6) (2024) 04024105, https://doi.org/10.1061/JMCEE7.MTENG-16964.

[5] H. Sadeghi, P. Alipanahi, Saturated hydraulic conductivity of problematic soils measured by a newly developed low-compliance triaxial permeameter, Eng. Geol. 278 (2020) 105827, https://doi.org/10.1016/j.enggeo.2020.105827.

[6] F. Arabchobdar, H. Sadeghi, M. Gholami, P. Alipanahi, Multi-directional deformation and hydraulic conductivity of expansive soils subjected to freeze–thaw cycles from three distinct initial saturation levels, J. Rock Mech. Geotech. Eng. (2024), https://doi.org/10.1016/j.jrmge.2024.10.007.

[7] S.D. Khadka, P.W. Jayawickrama, S. Senadheera, B. Segvic, Stabilization of highly expansive soils containing sulfate using metakaolin and fly ash-based geopolymer modified with lime and gypsum, Transp. Geotech. 23 (2020) 100327, https://doi.org/10.1016/j.trgeo.2020.100327.

[8] H. Sadeghi, A. Hasani Motlagh, A. Golaghaei Darzi, P. Alipanahi, S. Khodadadi, D. Song, Measurement and modeling of the saturated hydraulic conductivity functions of collapsible and expansive soils, Int. J. Geomech. 24 (4) (2024) 04024039, https://doi.org/10.1061/IJGNAI.GMENG-8788.

[9] F. Yazdani, H. Sadeghi, P. Alipanahi, M. Gholami, A.K. Leung, Evaluation of plant growth and spacing effects on bioengineered slopes subjected to rainfall, Biogeotechnics 2 (2) (2024) 100080, https://doi.org/10.1016/j.bgtech.2024.100080.

[10] A. Zarei, A. Hasani Motlagh, M. Hajialilue Bonab, P. Alipanahi, Influence of ground slope and relative density on liquefaction-induced lateral spreading: a physical modeling, Geotech. Geol. Eng. 42 (6) (2024) 5189–5208, https://doi.org/10.1007/s10706-024-02794-2.

[11] M.K. Atahu, F. Saathoff, A. Gebissa, Strength and compressibility behaviors of expansive soil treated with coffee husk ash, J. Rock Mech. Geotech. Eng. 11 (2) (2019) 337–348, https://doi.org/10.1016/j.jrmge.2018.11.004.

[12] S. Ahmad, M.S.A. Ghazi, M. Syed, M.A. Al-Osta, Utilization of fly ash with and without secondary additives for stabilizing expansive soils: a review, Results Eng. (2024) 102079, https://doi.org/10.1016/j.rineng.2024.102079.

[13] H.A. Chenarboni, S.H. Lajevardi, H. MolaAbasi, E. Zeighami, The effect of zeolite and cement stabilization on the mechanical behavior of expansive soils, Constr. Build. Mater. 272 (2021) 121630, https://doi.org/10.1016/j.conbuildmat.2020.121630.

[14] M. Khemissa, A. Mahamedi, Cement and lime mixture stabilization of an expansive overconsolidated clay, Appl. Clay Sci. 95 (2014) 104–110, https://doi.org/10.1016/j.clay.2014.03.017.

[15] Z. Gao, Y. Li, H. Qian, M. Wei, Environmental, economic, and social sustainability assessment: a case of using contaminated tailings stabilized by waste-based geopolymer as road base, Sci. Total Environ. 888 (2023) 164092, https://doi.org/10.1016/j.scitotenv.2023.164092.

[16] H. MolaAbasi, S.N. Semsani, M. Saberian, A. Khajeh, J. Li, M. Harandi, Evaluation of the long-term performance of stabilized sandy soil using binary mixtures: a micro- and macro-level approach, J. Clean. Prod. 267 (2020) 122209, https://doi.org/10.1016/j.jclepro.2020.122209.

[17] MolaAbasi, H. 2016. Laboratory Investigation on Mechanical Behavior of Babolsar sand Stabilized with Cement and Zeolite. Babol Noshirvani University of Technology.

[18] C. Le Quéré, R.M. Andrew, P. Friedlingstein, et al., Global carbon budget 2018, Earth Syst. Sci. Data 10 (4) (2018) 2141–2194, https://doi.org/10.5194/essd-10-2141-2018.

[19] T. Strunge, H. Naims, H. Ostovari, B. Olfe-Kräutlein, Priorities for supporting emission reduction technologies in the cement sector – a multi-criteria decision analysis of CO_2 mineralisation, J. Clean. Prod. 340 (2022) 130712, https://doi.org/10.1016/j.jclepro.2022.130712.

[20] M.S. Mamlouk, J.P. Zaniewski. Materials for Civil and Construction Engineers, Pearson, London, UK, 2014.

[21] E. Aprianti, P. Shafigh, S. Bahri, J.N. Farahani, Supplementary cementitious materials originating from agricultural wastes – A review, Constr. Build. Mater. 74 (2015) 176–187, https://doi.org/10.1016/j.conbuildmat.2014.10.010.

[22] M. Gholami, H. Sadeghi, P. Alipanahi, Anisotropic hydraulic conductivity of as-compacted, bare and vegetated soils, Géotechnique (2024) 1–40, https://doi.org/10.1680/jgeot.23.00248.

[23] H. Sadeghi, F.Y.B. Kohal, M. Gholami, P. Alipanahi, D. Song, Hydro-mechanical modeling of a vegetated slope subjected to rainfall, E3S Web Conf. 382 (2023) 13004, https://doi.org/10.1051/e3sconf/202338213004.

[24] Y. Wang, Y. Wang, C. Konstantinou, Strength behavior of temperature-dependent MICP-treated soil, J. Geotech. Geoenviron. Eng. 149 (12) (2023) 04023116, https://doi.org/10.1061/JGGEFK.GTENG-11526.

[25] K.K. Martin, H.K. Tirkolaei, E. Kavazanjian Jr., Field-scale EICP biocemented columns for ground improvement, J. Geotech. Geoenviron. Eng. 150 (8) (2024) 05024006, https://doi.org/10.1061/JGGEFK.GTENG-11635.

[26] F.M. Masrour, M.N. Mirsadeghi, H. MolaAbasi, R.J. Chenari, Effect of nanosilica on the macro- and microbehavior of dispersive clays, J. Mater. Civ. Eng. 33 (12) (2021) 04021349, https://doi.org/10.1061/(ASCE)MT.1943-5533.0003975.

[27] J. Wang, Y. Deng, C. Mou, J. Ding, J. Ni, X. Wan, Durability and degradation mechanisms of dredged clays stabilized with ternary geopolymer under cyclic drying–wetting environments, Bull. Eng. Geol. Environ. 84 (5) (2025) 1–9, https://doi.org/10.1007/s10064-025-04325-x.

[28] J. Ni, S. Liu, Y. Wang, G. Xu, Synergistic influence of lime and straw on dredged sludge reinforcement under vacuum preloading, Constr. Build. Mater. 421 (2024) 135642, https://doi.org/10.1016/j.conbuildmat.2024.135642.

[29] J. Wang, H. Wang, J. Ding, J. Ni, C. Mou, X. Wan, Investigation on performance improvement of dredged sediment with high water content stabilized with alkali-activated materials, J. Soils Sediments 24 (3) (2024) 1464–1473, https://doi.org/10.1007/s11368-023-03680-y.

[30] Y. Ma, L. Cheng, D. Zhang, F. Zhang, S. Zhou, Y. Ma, J. Guo, G. Zhang, B. Xing, Stabilization of Pb, Cd, and Zn in soil by modified zeolite: mechanisms and evaluation of effectiveness, Sci. Total Environ. 814 (2022) 152746, https://doi.org/10.1016/j.scitotenv.2021.152746.

[31] H. MolaAbasi, B. Kordtabar, A. Kordnaeij, Parameters controlling strength of zeolite–cement–sand mixture, Int. J. Geotech. Eng. 11 (1) (2017) 72–79, https://doi.org/10.1080/19386362.2016.1186412.

[32] S. Oruji, R. Khoshbin, R. Karimzadeh, Preparation of hierarchical structure of Y zeolite with ultrasonic-assisted alkaline treatment method used in catalytic cracking of middle distillate cut: the effect of irradiation time, Fuel Process. Technol. 176 (2018) 283–295, https://doi.org/10.1016/j.fuproc.2018.03.035.

[33] S. Waghmare, A. Katdare, N. Patil, Studies on computing compressive strength of zeolite blended concrete using multiple regression analysis, Mater. Today Proc 49 (2022) 1239–1245, https://doi.org/10.1016/j.matpr.2021.06.296.

[34] Ş. Öncü, H. Bilsel, Characterization of sand and zeolite stabilized expansive soil as landfill liner material under environmental and climatic effects, E3S Web Conf 195 (2020) 03034, https://doi.org/10.1051/e3sconf/202019503034.

[35] A.A. Sharo, F.M. Shaqour, J.M. Ayyad, Maximizing strength of CKD-stabilized expansive clayey soil using natural zeolite, KSCE J. Civ. Eng. 25 (4) (2021) 1204–1213, https://doi.org/10.1007/s12205-021-0786-2.

[36] Y.T. Tran, J. Lee, P. Kumar, K.H. Kim, S.S. Lee, Natural zeolite and its application in concrete composite production, Compos. Part B Eng. 165 (2019) 354–364, https://doi.org/10.1016/j.compositesb.2018.12.084.
[37] H. MolaAbasi, M. Saberian, A. Kordnaeij, J. Omer, J. Li, P. Kharazmi, Predicting the stress–strain behaviour of zeolite-cemented sand based on the unconfined compression test using GMDH type neural network, J. Adhes. Sci. Technol. 33 (9) (2019) 945–962, https://doi.org/10.1080/01694243.2019.1571659.
[38] M. Saberian, M.M. Khabiri, Effect of oil pollution on function of sandy soils in protected deserts and investigation of their improvement guidelines (case study: kalmand area, Iran), Environ. Geochem. Health 40 (2018) 243–254, https://doi.org/10.1007/s10653-016-9897-y.
[39] M. Ding, F. Zhang, X. Ling, B. Lin, Effects of freeze–thaw cycles on mechanical properties of polypropylene fiber and cement stabilized clay, Cold Reg. Sci. Technol. 154 (2018) 155–165, https://doi.org/10.1016/j.coldregions.2018.07.004.
[40] Y. Lu, S. Liu, Y. Zhang, Z. Li, L. Xu, Freeze–thaw performance of a cement-treated expansive soil, Cold Reg. Sci. Technol. 170 (2020) 102926, https://doi.org/10.1016/j.coldregions.2019.102926.
[41] R.J. Zhang, Y.T. Lu, T.S. Tan, K.K. Phoon, A.M. Santoso, Long-term effect of curing temperature on the strength behavior of cement-stabilized clay, J. Geotech. Geoenviron. Eng. 140 (8) (2014) 04014045, https://doi.org/10.1061/(ASCE)GT.1943-5606.0001144.
[42] A. Khajeh, S.A. Ebrahimi, H. MolaAbasi, R. Jamshidi Chenari, M. Payan, Effect of EPS beads in lightening a typical zeolite and cement-treated sand, Bull. Eng. Geol. Environ. 80 (11) (2021) 8615–8632, https://doi.org/10.1007/s10064-021-02458-1.
[43] A. Khaleque, M.M. Alam, M. Hoque, et al., Zeolite synthesis from low-cost materials and environmental applications: a review, Environ. Adv. 2 (2020) 100019, https://doi.org/10.1016/j.envadv.2020.100019.
[44] H. MolaAbasi, A. Khajeh, S. Naderi Semsani, Effect of the ratio between porosity and SiO_2 and al_2o_3 on tensile strength of zeolite-cemented sands, J. Mater. Civ. Eng. 30 (4) (2018) 04018028, https://doi.org/10.1061/(ASCE)MT.1943-5533.0002197.
[45] A.Q. Ahdal, M.A. Amrani, A.A.A. Ghaleb, A.A. Abadel, H. Alghamdi, M. Alamri, M. Wasim, M. Shameeri, Mechanical performance and feasibility analysis of green concrete prepared with local natural zeolite and waste PET plastic fibers as cement replacements. Case stud, Constr. Mater. 17 (2022) 01256, https://doi.org/10.1016/j.cscm.2022.e01256.
[46] H. MolaAbasi, I. Shooshpasha, Influence of zeolite and cement additions on mechanical behavior of sandy soil, J. Rock Mech. Geotech. Eng. 8 (5) (2016) 746–752, https://doi.org/10.1016/j.jrmge.2016.01.008.
[47] A.H. Motlagh, M. Hassanlourad, M. Hosseinzadeh, M. Bakhshy, Cyclic and monotonic mechanical behavior of heavy metal-contaminated clayey sand stabilized with zeolite, Bull. Eng. Geol. Environ. 84 (10) (2025) 1–21, https://doi.org/10.1007/s10064-025-04337-7.
[48] A.A. Shahmansouri, H.A. Bengar, H. AzariJafari, Life cycle assessment of eco-friendly concrete mixtures incorporating natural zeolite in sulfate-aggressive environment, Constr. Build. Mater. 268 (2021) 121136, https://doi.org/10.1016/j.conbuildmat.2020.121136.
[49] A.M. Osman, A. Al-Tabbaa, Effect of cement–zeolite grouts on the durability of stabilised clays, in: Proceedings of the 17th International Conference on Soil Mechanics and Geotechnical Engineering, 2009, pp. 3–6, https://doi.org/10.3233/978-1-60750-031-5-3.
[50] J.X. Shi, The applications of zeolite in sustainable binders for soil stabilization, Appl. Mech. Mater. 256 (2013) 112–115, https://doi.org/10.4028/www.scientific.net/AMM.256-259.112.
[51] E. Tabrizi, A.A. Dibazar, M. Hajialilue-Bonab, A. Esmatkhah Irani, A. Assadi-Langroudi, The partially drained behaviour of dense fibre-reinforced sands, Sustainability 15 (23) (2023) 16286, https://doi.org/10.3390/su152316286.
[52] M. Turkoz, P. Vural, The effects of cement and natural zeolite additives on problematic clay soils, Sci. Eng. Compos. Mater. 20 (4) (2013) 395–405, https://doi.org/10.1515/secm-2012-0104.
[53] H.R. Akbari, H. Sharafi, A.R. Goodarzi, Effect of polypropylene fiber inclusion in kaolin clay stabilized with lime and nano-zeolite considering temperatures of 20 and 40 °C, Bull. Eng. Geol. Environ. 80 (2021) 1841–1855, https://doi.org/10.1007/s10064-020-02028-x.
[54] H. MolaAbasi, P. Kharazmi, A. Khajeh, M. Saberian, R.J. Chenari, M. Harandi, J. Li, Low plasticity clay stabilized with cement and zeolite: an experimental and environmental impact study, Resour. Conserv. Recycl. 184 (2022) 106408, https://doi.org/10.1016/j.resconrec.2022.106408.
[55] W.S. Sarro, G.M. Assis, G.C.S. Ferreira, Experimental investigation of the UPV wavelength in compacted soil, Constr. Build. Mater. 272 (2021) 121834, https://doi.org/10.1016/j.conbuildmat.2020.121834.
[56] M.R. Khodayari, M.M. Ahmadi, Excess pore water pressure along the friction sleeve of a piezocone penetrating in clay: numerical study, Int. J. Geomech. 20 (7) (2020) 04020100, https://doi.org/10.1061/(ASCE)GM.1943-5622.0001724.
[57] A.E. Irani, M. Hajialilue-Bonab, A. Assadi-Langroudi, E.M. Tabrizi, Pore-pressure-dependent performance of rocking foundations, Soil Dyn. Earthq. Eng. 183 (2024) 108772, https://doi.org/10.1016/j.soildyn.2024.108772.
[58] M. Rahmati, V. Toufigh, K. Keyvan, Monitoring of crack healing in geopolymer concrete using a nonlinear ultrasound approach in phase-space domain, Ultrasonics 134 (2023) 107095, https://doi.org/10.1016/j.ultras.2023.107095.
[59] G. Suazo, A. Fourie, J. Doherty, Experimental investigation of propagation and transmission of compressional stress waves in cemented paste backfill, J. Geotech. Geoenviron. Eng. 143 (3) (2017) 04016104, https://doi.org/10.1061/(ASCE)GT.1943-5606.0001600.
[60] A.J. Choobbasti, M.A. Samakoosh, S.S. Kutanaei, Mechanical properties of soil stabilized with nano calcium carbonate and reinforced with carpet waste fibers, Constr. Build. Mater. 211 (2019) 1094–1104, https://doi.org/10.1016/j.conbuildmat.2019.03.306.
[61] N.C. Consoli, L. Festugato, H.C.S. Filho, G.D. Miguel, A.T. Neto, D. Andreghetto, Durability assessment of soil–pozzolan–lime blends through ultrasonic pulse velocity tests, J. Mater. Civ. Eng. 32 (8) (2020) 04020223, https://doi.org/10.1061/(ASCE)MT.1943-5533.0003298.
[62] Z. Su, J.M. Tinjum, A. Gokce, T.B. Edil, Freeze–thaw cycling effect on the constrained modulus and UCS of cementitiously stabilized materials, In: Pavement Materials, Structures, and Performance (2014) 364–374, https://doi.org/10.1061/9780784413418.036.
[63] T. Mandal, J.M. Tinjum, T.B. Edil, Non-destructive testing of cementitiously stabilized materials using ultrasonic pulse velocity test, Transp. Geotech. 6 (2016) 97–107, https://doi.org/10.1016/j.trgeo.2015.09.003.
[64] D.R. Biswal, U.C. Sahoo, S.R. Dash, Non-destructive strength and stiffness evaluation of cement-stabilised granular lateritic soils, Road Mater. Pavement Des. 21 (3) (2020) 835–849, https://doi.org/10.1080/14680629.2018.1511458.
[65] S. Subramanian, Q. Khan, T. Ku, Effect of sand on the stiffness characteristics of cement-stabilized clay, Constr. Build. Mater. 264 (2020) 120192, https://doi.org/10.1016/j.conbuildmat.2020.120192.
[66] J. Li, F. Xiao, L. Zhang, S.N. Amirkhanian, Life cycle assessment and life cycle cost analysis of recycled solid waste materials in highway pavement: a review, J. Clean. Prod. 233 (2019) 1182–1206, https://doi.org/10.1016/j.jclepro.2019.06.061.
[67] A.J. Raymond, J.T. DeJong, A. Kendall, J.T. Blackburn, R. Deschamps, Life cycle sustainability assessment of geotechnical ground improvement methods, J. Geotech. Geoenviron. Eng. 147 (12) (2021) 04021161, https://doi.org/10.1061/(ASCE)GT.1943-5606.0002646.
[68] L.J. Rodriguez, P. Peças, H. Carvalho, C.E. Orrego, A literature review on life cycle tools fostering holistic sustainability assessment: an application in biocomposite materials, J. Environ. Manag. 262 (2020) 110308, https://doi.org/10.1016/j.jenvman.2020.110308.
[69] F. Yazdani, P. Alipanahi, H. Sadeghi, A comparative study of environmental and economic assessment of vegetation-based slope stabilization with conventional methods, J. Environ. Manag. 359 (2024) 121002, https://doi.org/10.1016/j.jenvman.2024.121002.
[70] S. Harris, G. Tsalidis, J.B. Corbera, J.J. Gallart, F. Tegstedt, Application of LCA and LCC in the early stages of wastewater treatment design: a multiple case study of brine effluents, J. Clean. Prod. 307 (2021) 127298, https://doi.org/10.1016/j.jclepro.2021.127298.
[71] H. Sadeghi, M. Gholami, P. Alipanahi, D. Song, The influence of isotropic loading and unloading on anisotropic evolution of saturated hydraulic conductivity of bentonite–sand mixtures in a cube triaxial permeameter, Eng. Geol. 331 (2024) 107454, https://doi.org/10.1016/j.enggeo.2024.107454.
[72] G. Liu, T. Gu, P. Xu, J. Hong, A. Shrestha, I. Martek, A production line-based carbon emission assessment model for prefabricated components in China, J. Clean. Prod. 209 (2019) 30–39, https://doi.org/10.1016/j.jclepro.2018.10.172.
[73] E.B. Tutuş, O. Pekcan, M. Altun, M. Türkezer, Optimizing reinforced cantilever retaining walls under dynamic loading using improved flower pollination algorithm. Applications of Flower Pollination Algorithm and Its Variants, Springer, Singapore, 2021, pp. 139–169.
[74] Z. Zhang, R. Li, S. Lian, Z. Jiang, Q. Liu, C. Song, Energy, economic and environment assessment of membrane–cryogenic hybrid recovery propane process – process simulation and life cycle assessment, J. Clean. Prod. 391 (2023) 136146, https://doi.org/10.1016/j.jclepro.2023.136146.
[75] X. Yuan, Y. Tang, Y. Li, Q. Wang, J. Zuo, Z. Song, Environmental and economic impacts assessment of concrete pavement brick and permeable brick production process – a case study in China, J. Clean. Prod. 171 (2018) 198–208, https://doi.org/10.1016/j.jclepro.2017.10.037.
[76] H.H. Ghayeb, H.A. Razak, N.R. Sulong, Evaluation of the CO_2 emissions of an innovative composite precast concrete structure building frame, J. Clean. Prod. 242 (2020) 118567, https://doi.org/10.1016/j.jclepro.2019.118567.
[77] C. Mao, Q. Shen, L. Shen, L. Tang, Comparative study of greenhouse gas emissions between off-site prefabrication and conventional construction methods: two case studies of residential projects, Energy Build. 66 (2013) 165–176, https://doi.org/10.1016/j.enbuild.2013.07.033.
[78] Y. Tang, Y. Li, Y. Shi, Q. Wang, X. Yuan, J. Zuo, Environmental and economic impacts assessment of prebaked anode production process: a case study in Shandong Province, China. J. Clean. Prod. 196 (2018) 1657–1668, https://doi.org/10.1016/j.jclepro.2018.06.121.
[79] A. Suddeepong, A. Intra, S. Horpibulsuk, C. Suksiripattanapong, A. Arulrajah, J. S. Shen, Durability against wetting–drying cycles for cement-stabilized reclaimed asphalt pavement blended with crushed rock, Soils and Foundations 58 (2) (2018) 333–343, https://doi.org/10.1016/j.sandf.2018.02.006.
[80] J. Pooni, F. Giustozzi, D. Robert, S. Setunge, B.J. O'Donnell, Durability of enzyme-stabilized expansive soil in road pavements subjected to moisture degradation, Transp. Geotech. 21 (2019) 100255, https://doi.org/10.1016/j.trgeo.2019.100255.